# CHAPTER 4

# GROUNDWATER FLOW AND SOLUTE TRANSPORT MODELS

This chapter presents the development of groundwater flow and contaminant transport models of the contaminated aquifers in the study area. The models can be used to assess groundwater contamination in the study area and, subsequently, design the remediation scheme for the site if necessary. The model setup involves several steps that include site conceptual model construction, model design, model calibration, and the sensitivity analysis of the optimized parameters. Results of groundwater flow model show the pattern and direction of groundwater flow and can be used to construct the solute transport model. The result of the calibrated solute transport model will show the distribution of contaminants in the contaminated unconfined aquifers.

## 4.1 Site Conceptual Model

Conceptual model is an idealized summary and integration of available data, such as geology, hydrogeology, and hydrology for the study area, into a coherent representation of the flow system to be modeled. The conceptual model was usually documented using graphical representations and descriptive text before initiating model construction, execution, and calibration. The site conceptual model of the study area is shown in Figure 4.1.

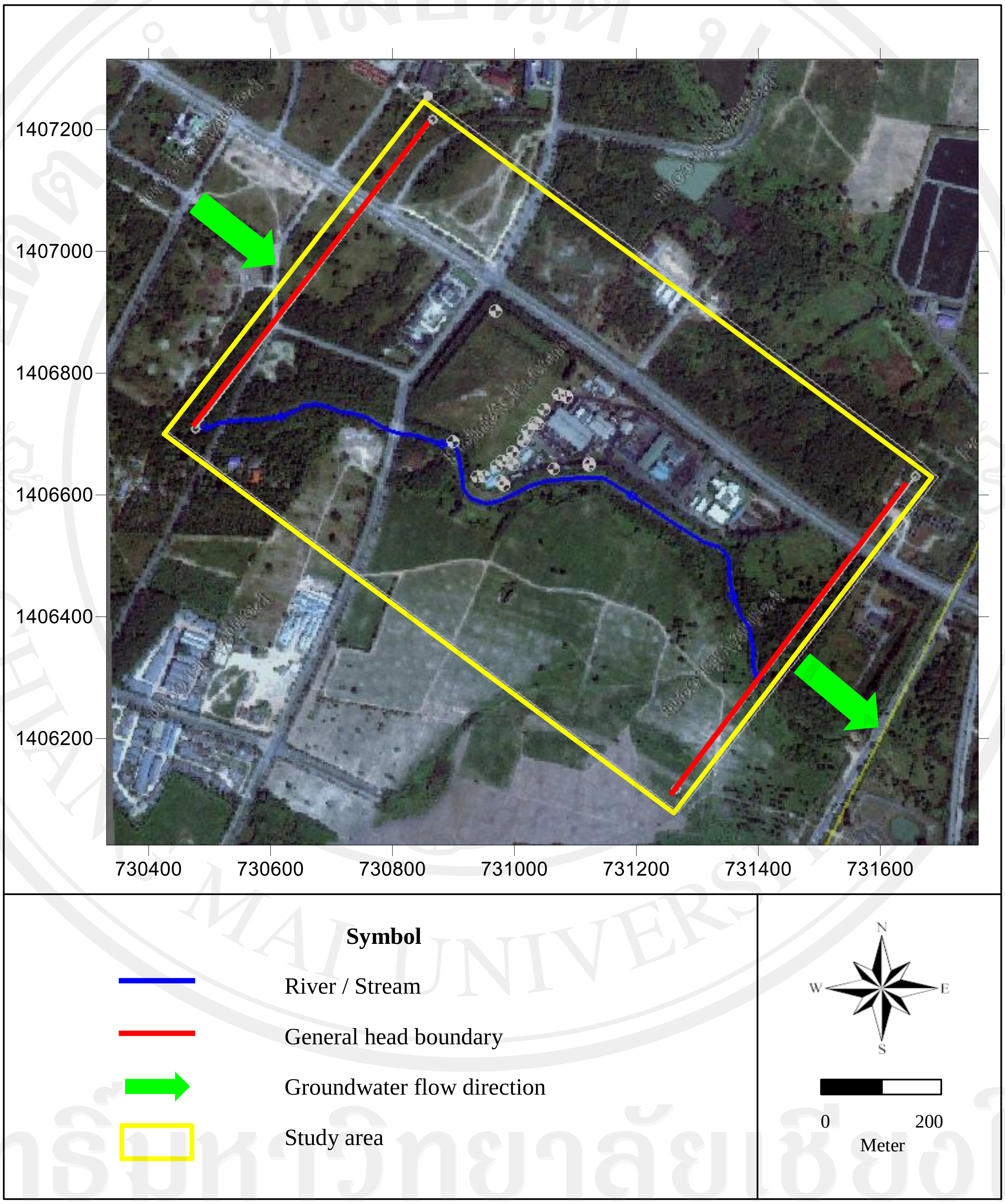


Figure 4.1 The conceptual model of the study area.

Base on hydrogeologic characterization of the study area described in Chapter 3, aquifer materials are divided into six hydrostratigraphic units where two sand units are main shallow unconfined aquifers. Clay unit in the study area can be considered as an aquitard layer and fractured Granite unit is the bedrock. General trend of groundwater flow direction of the study area is from northwest to southeast direction. This groundwater flow direction conforms to the flow direction of the main stream in the study area, Khong Chak Mak.

Figure 4.1 shows the site boundary and the general head boundary conditions of the conceptual model for flow model. The general head boundary (GHB) is used to simulate head-dependent recharge or discharge across an aquifer boundary in MODFLOW simulation. The general head boundary lines are in the northwest and southwest boundary of the conceptual model. These lines have the same value of hydraulic head along the line and hydraulic head of the northwest line is different from the southwest line. The blue line represents the river boundary condition (RIV) which takes in to account for simulating water exchange between aquifer and the running surface water. Natural recharge and evapotranspiration appears to be minimal in the study area since most of the area is paved with cement or asphalt. There is no record of groundwater extraction through wells within or near by the study area. Thus, neither (point/areal) source nor sink of groundwater is necessary in this simulation.

In the construction of a conceptual model for the *solute transport model*, contaminant source zones were postulated based on the site history review. Two source zones were located within the disposal site area near well no. 7 and in the liquid waste pond near well no. 3 (see Figure 4.2). The exact VOCs concentrations in the source zone are however unknown parameters and will be determined during model calibration process. Source zone no. 1 (near well no. 7) was estimated to begin leaking in 1990 prior to the completion of the lining construction. Source zone no.2 is the liquid waste pond that was constructed in 2000 after the disposal site had been operated for ten years. The concentrations of PCE and TCE in both sources were conceptualized and shown in Figure 4.2. These graphs show the concentration of source zone that started from zero and increased to the maximum levels of concentration and maintained in these levels until the end of the simulation time. The exact time-concentration curves for the source zones will be determined later in the model calibration process.

**4.2 Model Design**

This step involves the design of a model grid size, number of rows, columns, layers, and the associated model parameters. Each of the grid blocks requires the assignment of value of hydrogeologic properties such as hydraulic conductivities, dispersivities, porosities, and hydraulic conductance of river and general-head boundaries. The mathematical models used to simulate groundwater flow and solute transport are MODFLOW (Harbaugh et al., 2000) and RT3D (Clement, 1997), respectively.

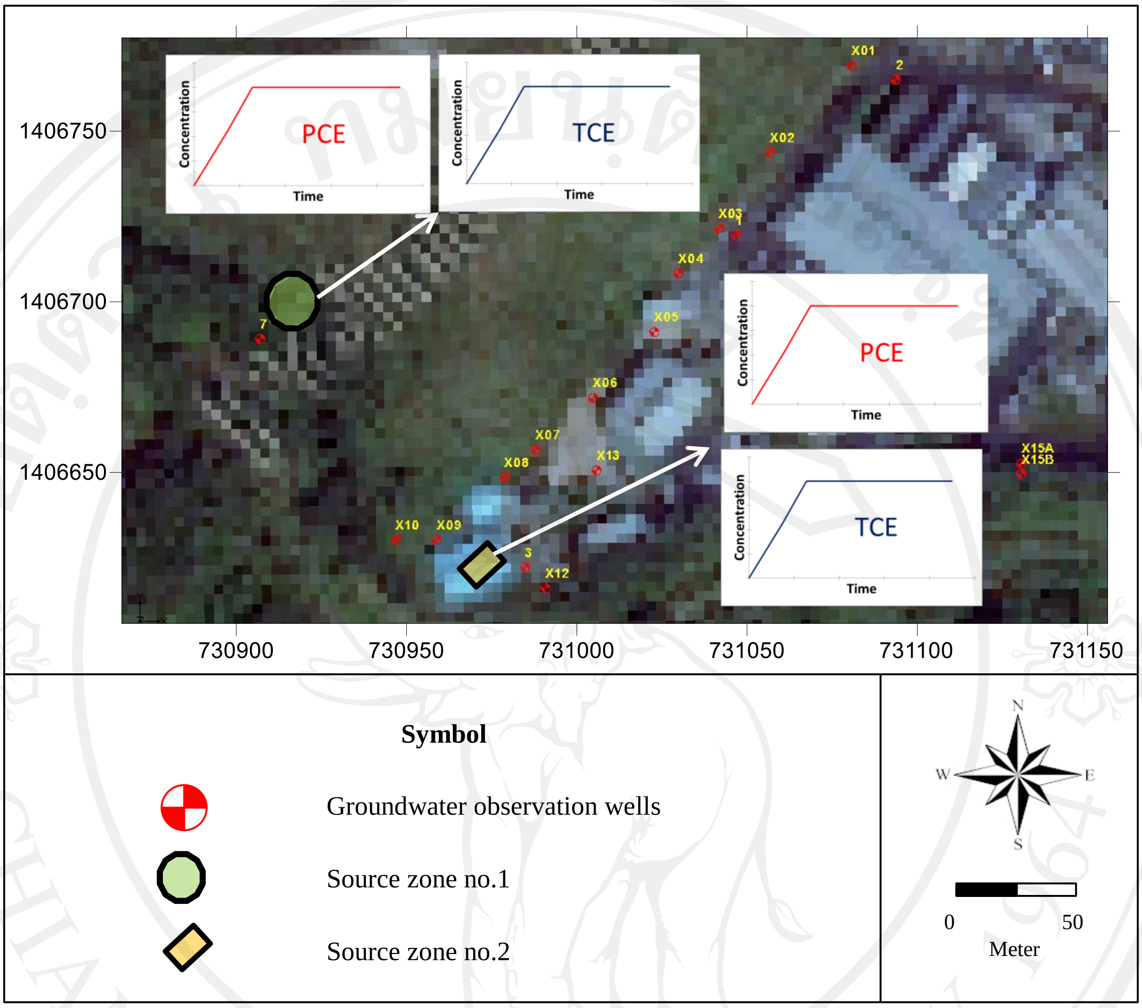


Figure 4.2 The source zone for the solute transport simulation of the study area (Note that the time-concentration of the source zone is only for illustrative purpose).

### 4.2.1 Model Grids and Layers

The study area was discretized, using GMS® software, into a non-uniform finite-difference grid of 127 columns, 131 rows, 15 layers covering the area of approximately 1010 × 660 $m^2$ and the maximum non-uniform depth of approximately 30 m (Figures 4.3 and 4.4).

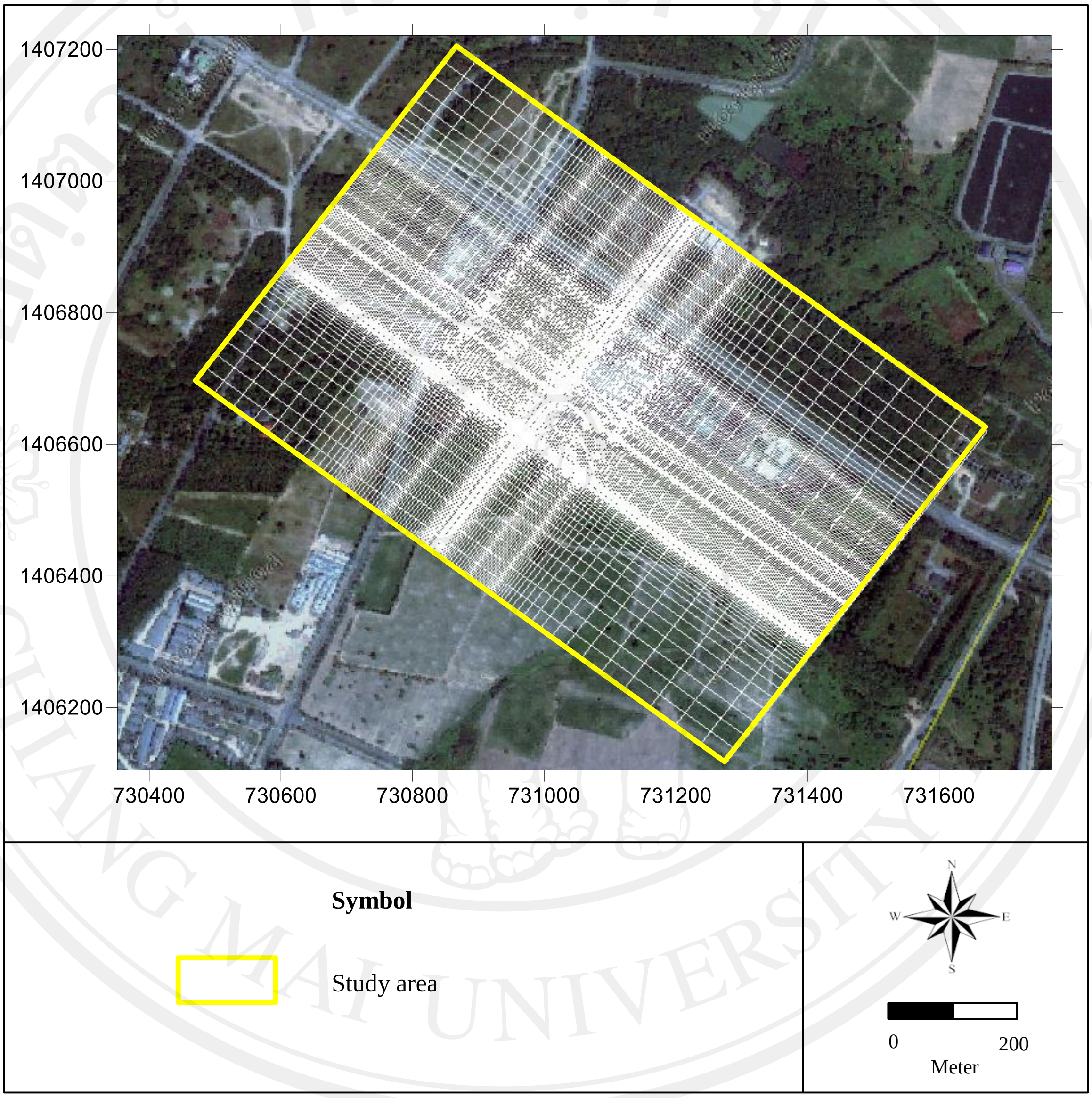


Figure 4.3 Non-uniform finite-difference grid of the study area.

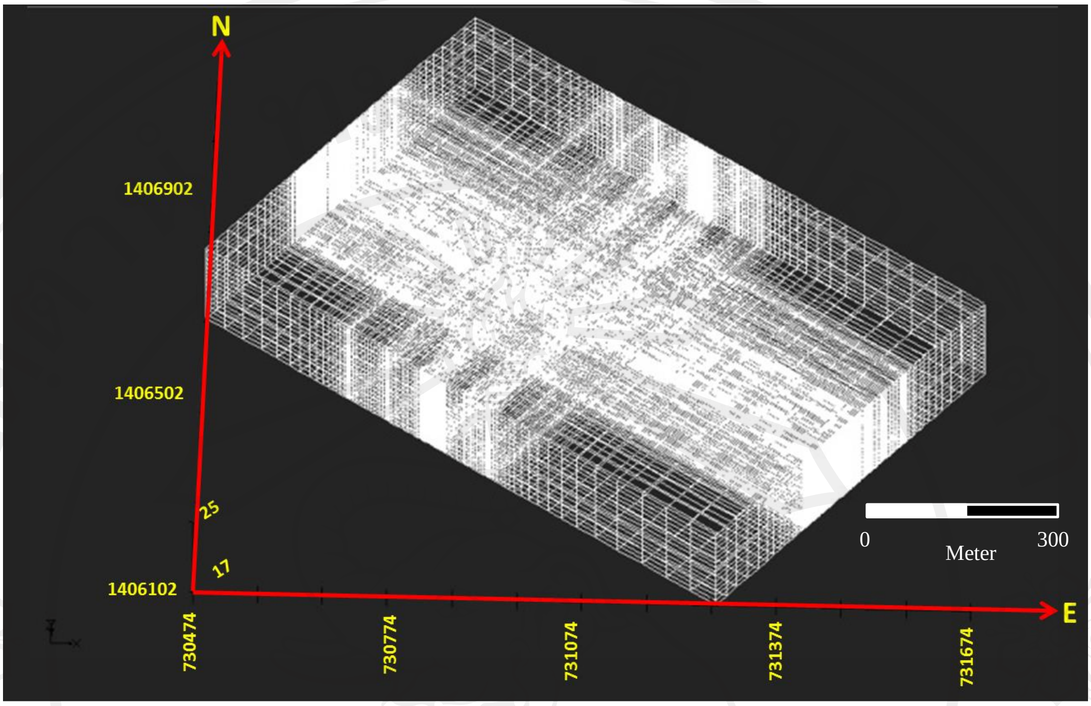


Figure 4.4 Non-uniform finite-difference grid of the study area show 127 lows, 131 columns, and 15 layers in oblique view. (Z-magnification is 5)

In the assignment of aquifer materials (total of six materials), the grid overlay option was used. In this method, each vertical column of cells intersects a vertical axis through the cell center and finds the highest and lowest intersection, i.e., the top and bottom of the entire set of solids. These elevations become the top and bottom elevation of the entire grid. The elevations of any intermediate layer boundaries are then linearly interpolated between these two extremes. The material properties are then assigned by computing the *x*-, *y*-, and *z*-coordinates of the center of each cell and determining which solid encloses the cell center. The material properties from that solid are then assigned to the cell. The result of grid overlay in this study is shown in Figures 4.5, 4.6, and 4.7.

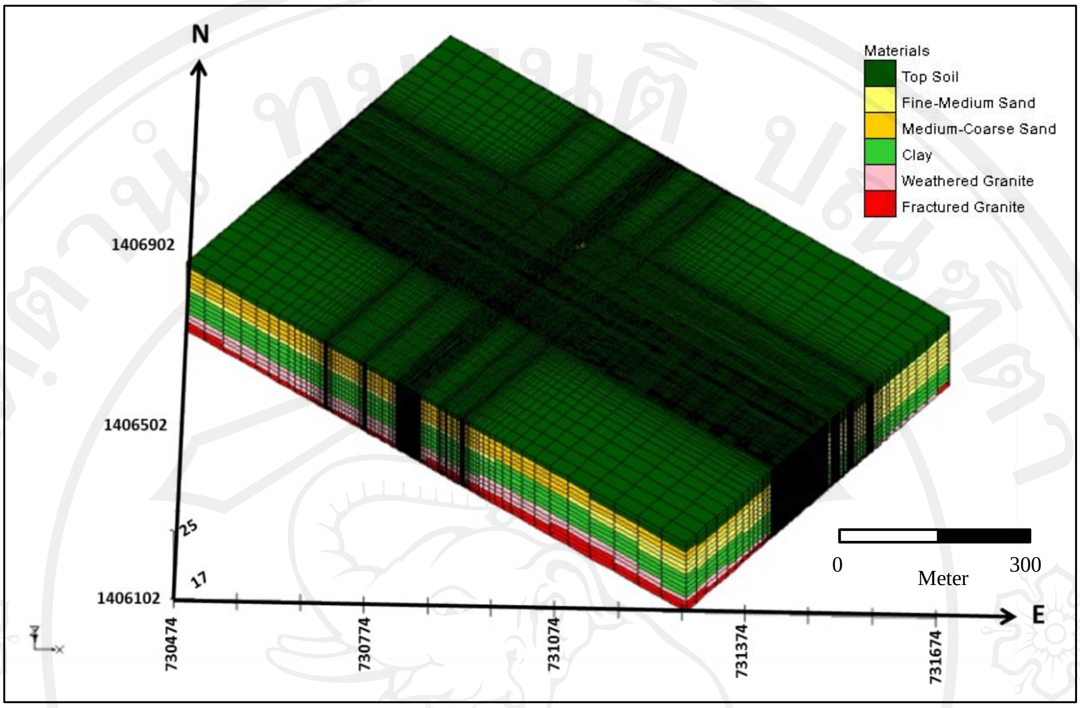


Figure 4.5 Non-uniform finite-difference grid with the solid model by grid overlay option in GMS® (oblique view).

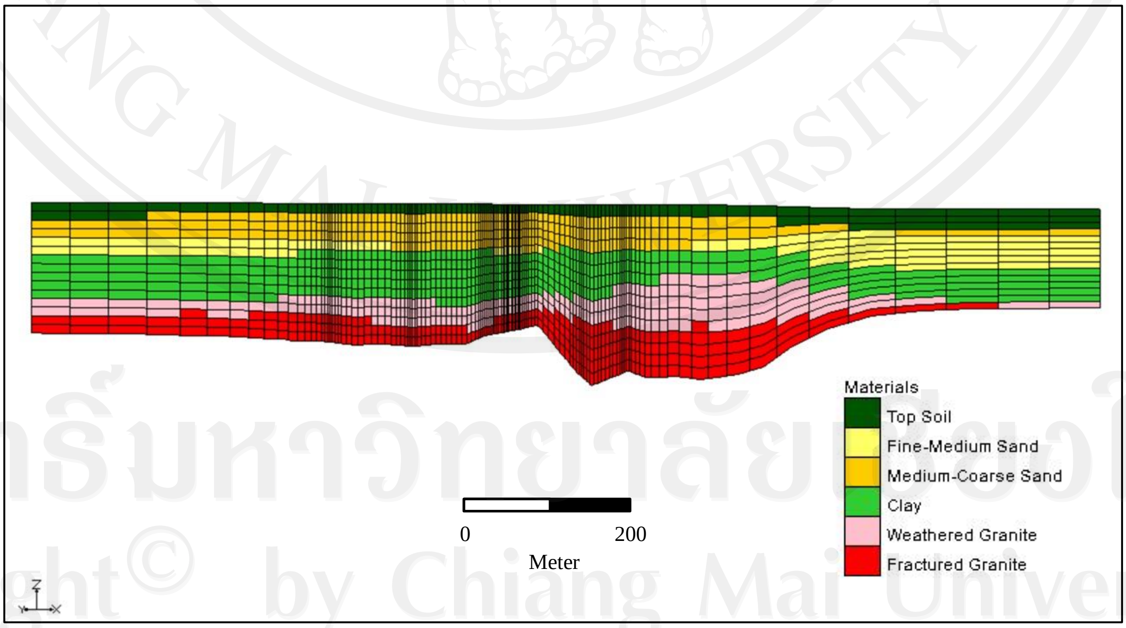


Figure 4.6 Non-uniform finite-difference grid with the solid model by grid overlay option in GMS® (cross at row no. 85).

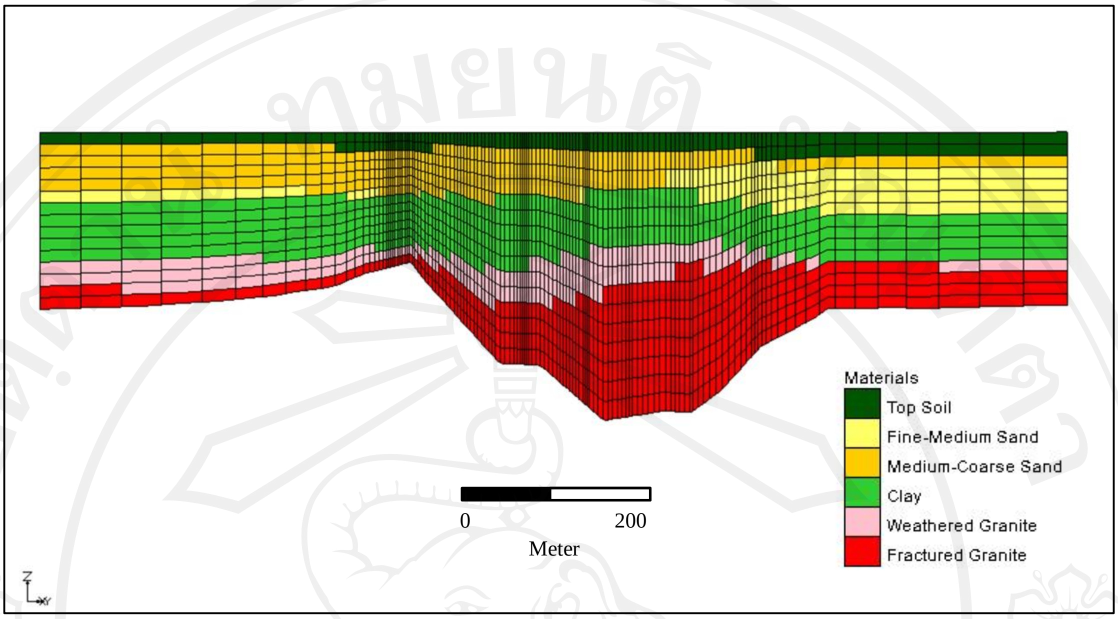


Figure 4.7 Non-uniform finite-difference grid with the solid model by grid overlay option in GMS® (cross at column no. 85).

### 4.2.2 Model Parameters

Hydraulic properties used in this study include horizontal hydraulic conductivity ($K_h$), vertical hydraulic conductivity ($K_v$), horizontal anisotropy, vertical anisotropy ($K_h / K_v$), porosity ($n$), and dispersivities ($a$). Horizontal hydraulic conductivity ($K_h$) in this study is the main parameter that is used in the groundwater flow simulation. Horizontal hydraulic conductivity controls the rate of groundwater flow through a unit of an aquifer at a given hydraulic gradient. In this study can divide the hydrogeologic units into six units, which have different values of $K_h$. Values of $K_h$ (Table 4.1) that are used in the groundwater flow model from Domenico and Schwartz (1990).

Table 4.1 Values of hydraulic conductivity for hydrogeologic unit in the study area. (Domenico and Schwartz, 1990)

| Hydrogeologic Unit | Hydraulic conductivity | |
|---|---|---|
| | Minimum (m/d) | Maximum (m/d) |
| Top soil | $8.6 \times 10^{-5}$ | 1.728 |
| Fine-Medium Sand | 0.0173 | 43.2 |
| Medium-Coarse Sand | 0.0778 | 518.4 |
| Clay | $8.64 \times 10^{-7}$ | $3.46 \times 10^{-4}$ |
| Weathered Granite | 0.2851 | 4.4928 |
| Fractured Granite | $6.91 \times 10^{-4}$ | 25.92 |

Another parameter used in the groundwater flow simulation is hydraulic conductance of the riverbed and general head boundary materials. MODFLOW uses the conductance to determine the amount of water that flows in or out of the model due to the boundary condition stresses. In the case of a river boundary condition, the conductance is defined in MODFLOW as the hydraulic conductivity of the river bed materials divided by the vertical thickness (length of travel based on vertical flow) of the river bed materials, multiplied by the area (width times the length) of the river in the cell. The last term, area, is the hardest parameter to determine by hand since it varies from cell to cell. However, GMS® can automatically calculate the conductance from equation (4.1),

$$C = \frac{K}{b} l_w , \tag{4.1}$$

where $C$ is conductance,

$K$ is hydraulic conductivity,

$b$ is thickness of the material in the direction of flow,

$l_w$ is the cross-sectional area perpendicular to the flow direction.

Parameters used in the solute transport simulation include longitudinal dispersivity ($a_L$), ratio of horizontal transverse dispersivity to longitudinal dispersivity (TRPT or $a_{T,H}/a_L$), ratio of vertical transverse dispersivity to longitudinal dispersivity (TRVT or $a_{T,V}/a_L$), degradation rate ($k$), and yield coefficient ($Y$). All these parameters, except for $Y$ (from known stoichiometry), will be obtained from model calibration processes. However, initial estimates of longitudinal dispersivities or $a_L$ were obtained from field tracer test conducted during site characterization processes.

### 4.3 Model Calibration

Model calibration is the process that the parameters of model are adjusted within realistic limits to produce the best match between simulated and measured data. Calibration requires that field conditions be properly characterized. Lack of proper characterization may result in a calibration to a set of conditions that do not represent actual field conditions. Since some input data are highly variable, sometimes suspected, and the data is limited. These values are typically adjusted and extrapolated through an iterative process until an acceptable match is made. When the best calibrated match is achieved, a final input data set should be established and demonstrated to be reasonable and realistic. There is no universally accepted goodness of fit criteria that apply in all cases. However, it is important that the modeler make every attempt to minimize the difference between model simulated and field conditions (Ohio EPA, 2007).

The systematic parameter estimation based on the non-linear least-square regression procedure was used to obtain the mass transfer parameters as well as the hydraulic properties of the aquifers. The goal of regression is to estimate unknown parameter values, so that the model produces calculated concentration values close to the field observation values. This is achieved by minimizing sum of squared residuals between measured and simulated values. Sum of squared weight residuals is sometimes called an objective function,

$$F = \sum_{i=1}^{N} w_i (h_i - \tilde{h}_i)^2 , \tag{4.2}$$

where F is the objective function,

$w$ is the weight which is inversely proportional to the variance of the observation,

$h_i$ is the simulated value of hydraulic head,

$\tilde{h}_i$ is the observation value of hydraulic head.

Model calibration in this study was done by using PEST to estimated parameters and calibrated these parameters. PEST is a non-linear parameter estimation package developed by Doherty (1994). The non-linear regression is solved by minimizing a weighted least square objective function with respect to the parameter values using a modified Gauss-Newton method. Parameter sensitivities are calculated using the perturbation method based on forward, backward, or central difference methods. In PEST, optimum parameter values can be constrained to lie between individually-specified upper and lower bounds. This is implemented using a mathematically advanced algorithm that actually regularizes the parameter estimation problem as bounds are imposed.

Sensitivity analysis can be used in the initial model parameterization process to investigate which parameters are sensitive with respect to the available observations, and which are insensitive and can be set to fixed values. PEST provides an independent sensitivity analysis module by adjusting model inputs, running the model, reading the outputs of interest, recording their values, and recommencing the computing cycle. However, the results of such an analysis should be carefully interpreted. The dimensionless, scaled sensitivities depends on the parameter values, and hence sensitivity statistics evaluated at some initial parameter values may be very different from the statistics obtained using other parameter sets (Hill, 1998). In addition, sensitivity statistics do not properly account for parameter correlations, implying that parameters that seem to be insensitive may have important correlations with other parameters that are essential for the model behavior (Madsen et al., 2002). For example, sensitivity of parameter $P$ can be found by equation:

$$\frac{\partial \Phi}{\partial P} = \frac{\Phi(P + \Delta P) - \Phi(P)}{\Delta P}. \tag{4.3}$$

## 4.4 Simulation Results

### 4.4.1 Groundwater Flow Simulation Results

From the model calibration stage, there are fourteen parameters which got from the parameter estimation process. These parameters include horizontal hydraulic conductivities $K_h$ of six units (Top soil, Fine-Medium Sand, Medium-Coarse Sand, Clay, Weathered Granite, and Fractured Granite), vertical anisotropy, conductance of river (five points), and conductance of the general head boundary (northwest boundary and southeast boundary). Estimated values of all parameter show in Table 4.2 and result from PEST program show in Appendix C. These results show most hydraulic conductivity values are in the reference range except the $K_h$ of Weathered Granite unit that in the study area has lower value than the reference range.

The result of groundwater flow simulation after the calibration process is shown in Figures 4.8. This simulation use parameters from Table 4.2 and generated contour of the hydraulic head in the study area. Figure 4.8 shows the result of hydraulic head at layer no. 3 of the groundwater flow model. Based on these results, this section of Khong Chak Mak appears to be a losing stream. Equipotential lines show that the stream loses water to the aquifer. The simulation result shows the main groundwater flow direction of the study area is from northwest to southeast.

Table 4.2 Estimated values and relative sensitivity values of all parameter from parameter estimation of groundwater flow simulation process.

| Parameter | | Estimated Value | Relative Sensitivity |
|---|---|---|---|
| Hydraulic Conductivity [m/d] | TopSoil Unit | 0.26129 | 0.5896 |
| | Fine-Medium Sand Unit | 1.3303 | 1.0000 |
| | Medium-Coarse Sand Unit | 9.7799 | 0.0140 |
| | Clay Unit | 1.66E-06 | 0.1229 |
| | Weathered Granite Unit | 2.51E-06 | 0.1568 |
| | Fractured Granite Unit | 3.1453 | 0.0027 |
| Vertical Anisotropy | | 18.586 | 0.0789 |
| River Conductance 1 [($m^2$/d)/m] | | 218.15 | 0.0033 |
| River Conductance 2 [($m^2$/d)/m] | | 152.05 | 0.0033 |
| River Conductance 3 [($m^2$/d)/m] | | 184.68 | 0.0037 |
| River Conductance 4 [($m^2$/d)/m] | | 71.227 | 0.0020 |
| River Conductance 5 [($m^2$/d)/m] | | 136.19 | 0.0234 |
| General Head Boundary Conductance NW [($m^2$/d)/m] | | 2273.1 | 0.0034 |
| General Head Boundary Conductance SE [($m^2$/d)/m] | | 2538.6 | 0.0025 |

Sensitivity analysis of groundwater flow simulation in this study was calculated using PEST (Table 4.2). The most sensitive parameters are hydraulic conductivities whereas the conductances have smaller impact or effect to the flow simulation. The most sensitive parameter is horizontal hydraulic conductivity of Fine-to-Medium Sand Unit because of this unit is the main of shallow unconfined aquifer within which most of observation wells are located.

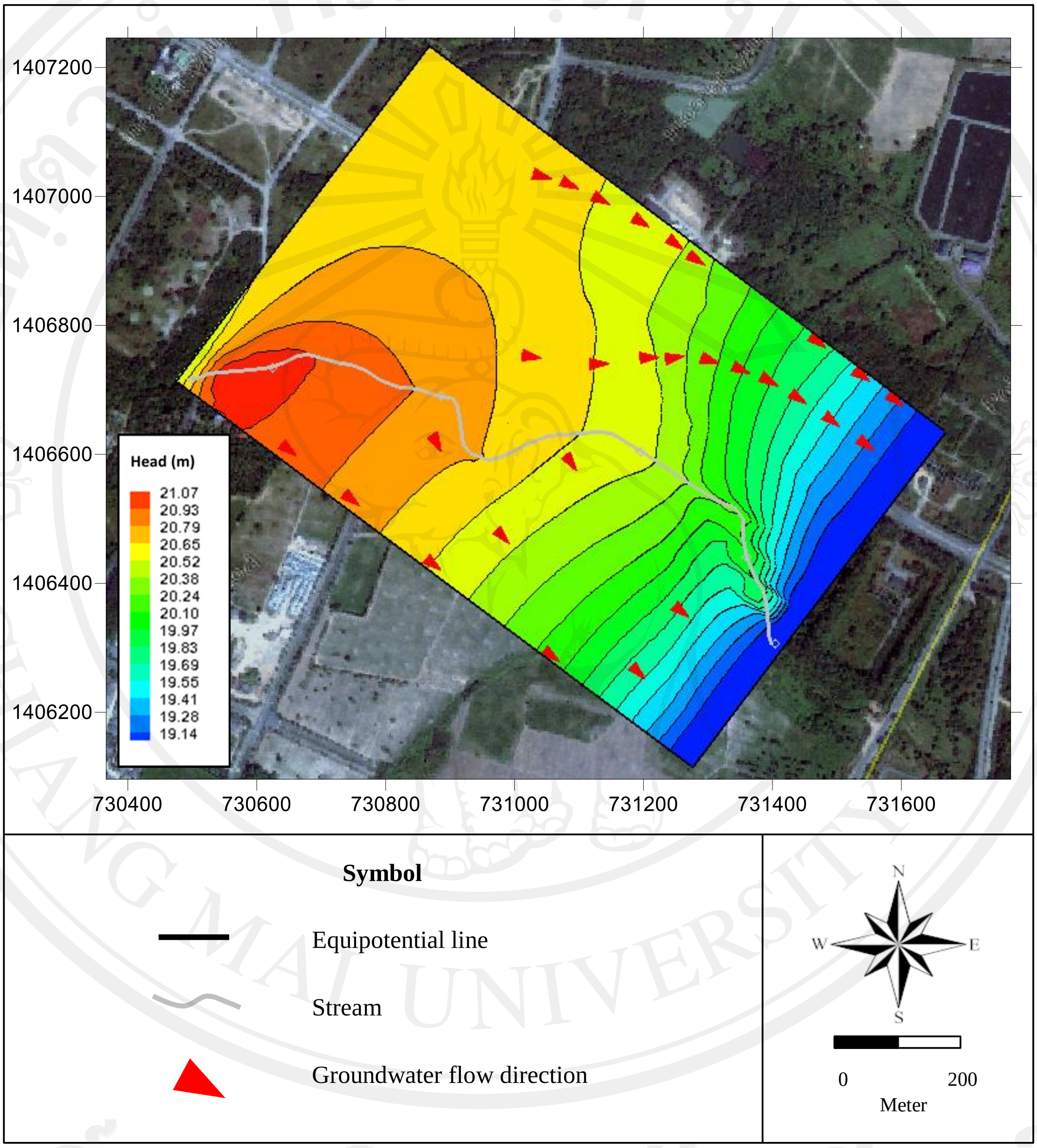


Figure 4.8 Hydraulic head from the groundwater flow simulation at layer no. 3.

**4.4.2 Solute Transport Simulation Results**

In the parameter estimation process, parameter values obtained from this process include porosity ($n$) and longitudinal dispersivity ($a_L$) of all hydrogeologic units, degradation rate of VOCs (PCE, TCE, DCE and VC), and concentration of PCE and TCE in two source zones. Estimated parameter values are shown in Table 4.3 and the result from PEST is shown in Appendix D.

The observed concentration of PCE, TCE, and *cis*-DCE in monitoring wells no. 1, 2, 3, and 7 were plotted against the simulated concentrations as shown in Figure 4.9. This represents the best estimated solute transport model achieved automatically by the aid of PEST program. In such plot, the average concentration refers to the flux-average VOC concentration from multiple grid blocks intersected by a well. On the other hand, the maximum concentration refers to the maximum VOC concentration found in any grid block among all grid blocks that well intersects.

Optimized parameter values obtained from the parameter estimation process were then used to simulate the solute transport model of this study area (i.e., prediction). This simulation starts from 1990 and finishes in 2010. Results of solute transport simulation illustrating plumes of PCE, TCE, and *cis*-DCE in layer no. 3 of the model are shown in Figures 4.10- 4.15.

From these results, dissolve VOCs plume have not migrated significantly far source zones except the case of DCE that show the largest plume size because the degradation rate of TCE is high. This finding agrees with groundwater geochemistry data and geomicrobiology observation (DEQP, 2010). Sensitivity analysis of the solute transport simulation (Table 4.3) indicates all parameters' sensitivity is in the same order of magnitude although that the degradation rate constant appears to be the most sensitive parameter in the model.

Table 4.3 Estimated parameter values and relative sensitivity of all parameter from parameter estimation of solute transport simulation process.

| Parameter | | | Estimated Value | Relative Sensitivity |
|---|---|---|---|---|
| Porosity (*n*) | | | 0.3 | 0.9084 |
| Longitudinal Dispersivity ($\alpha_L$) | | | 1.0 | 0.4366 |
| Degradation Rate (*k*) | Tetrachloroethene (PCE) | | 0.003 | 1.0000 |
| | Trichloroethene (TCE) | | 0.0085 | 0.8096 |
| | 1,2 Dichloroethene (DCE) | | 0.0005 | 0.9079 |
| | Vinyl Chloride (VC) | | 0.003 | 0.6106 |
| Source Concentration | Source no.1 | PCE | 6.5 | 0.6358 |
| | | TCE | 15.5 | 0.4850 |
| | Source no.2 | PCE | 0.007 | 0.5870 |
| | | TCE | 0.25 | 0.4662 |

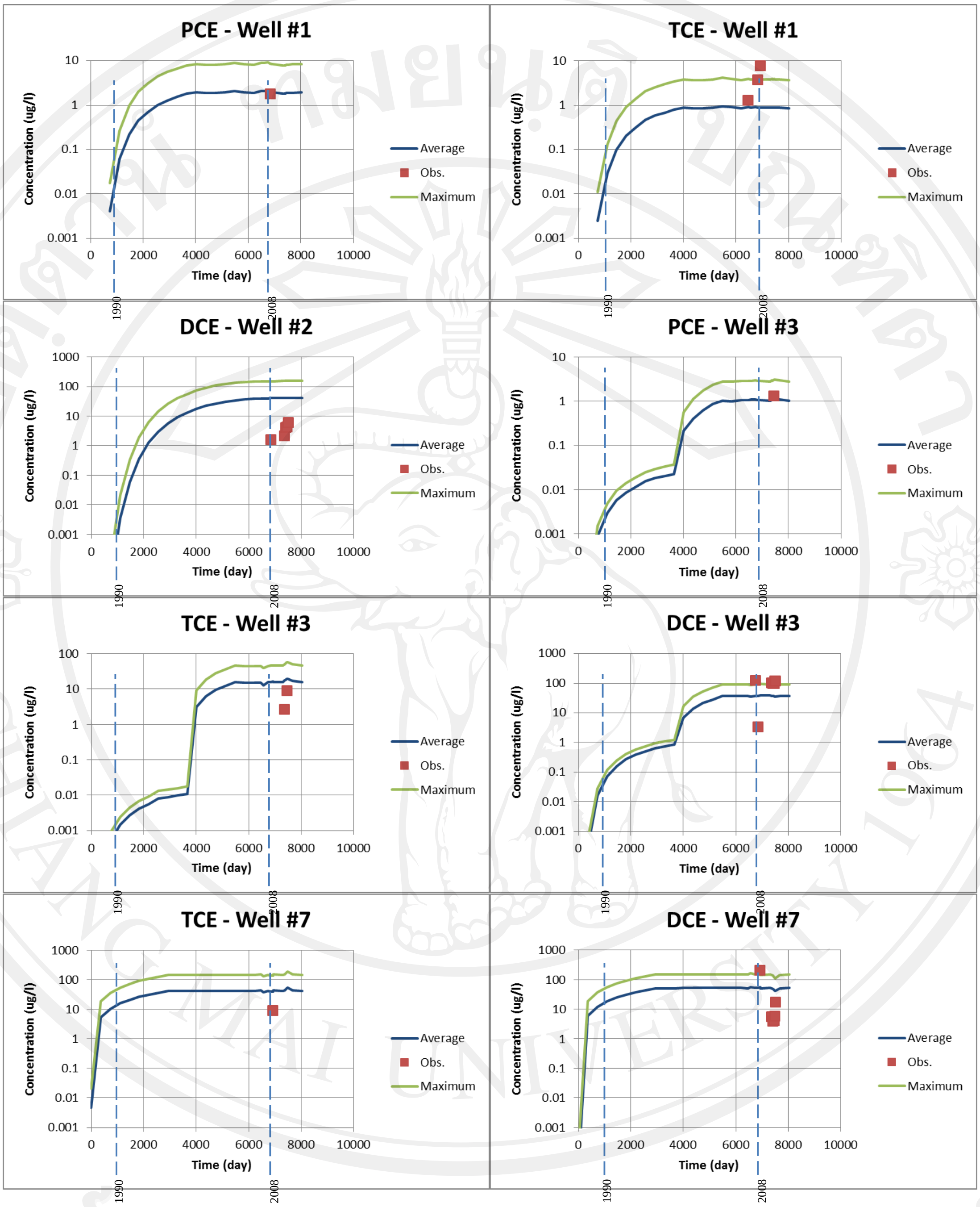


Figure 4.9 Graphs of the results from solute transport simulation compare with the observation data.

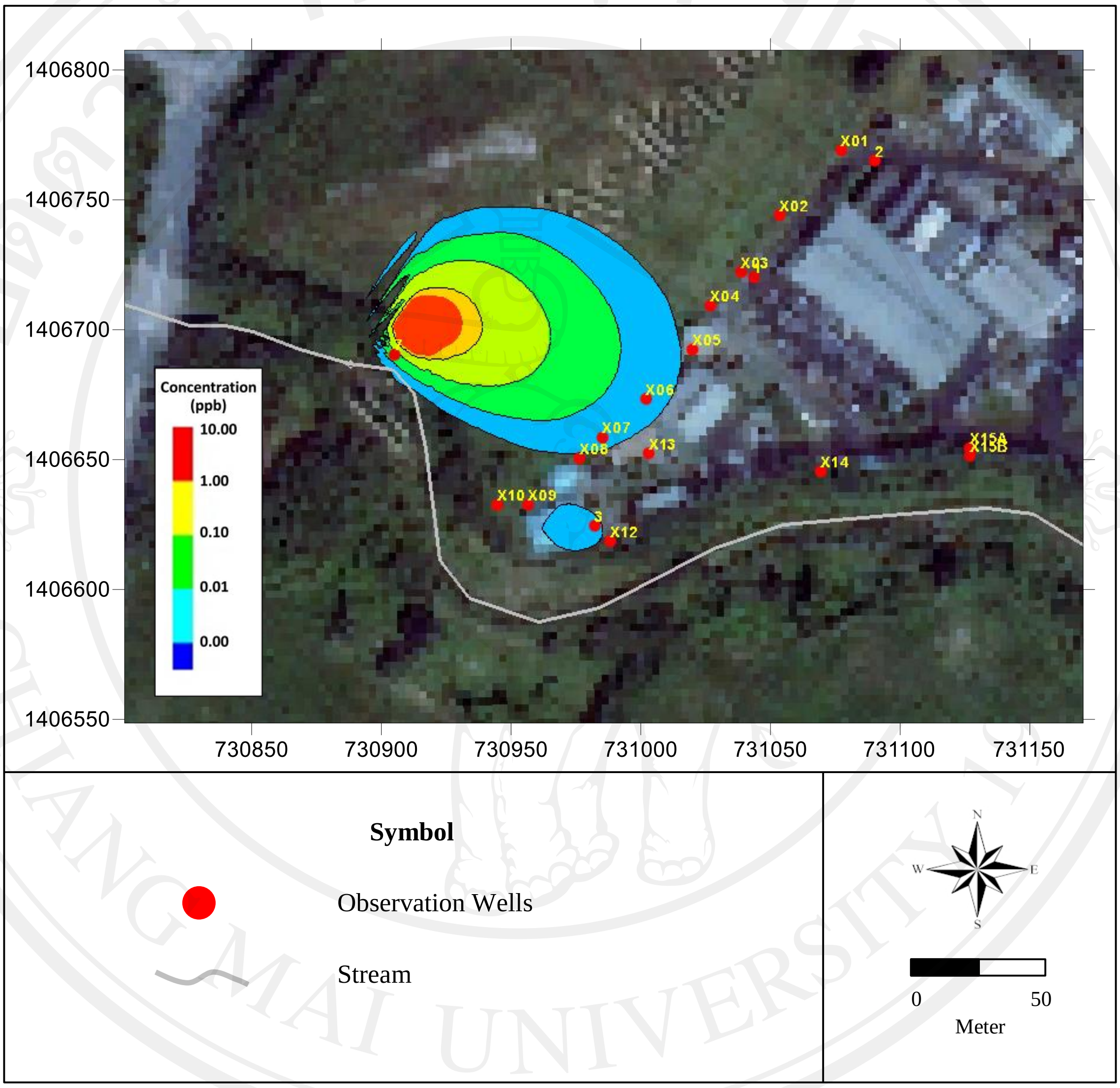


Figure 4.10  Plumes of PCE at the simulated time 27/12/2008 in layer no.3.

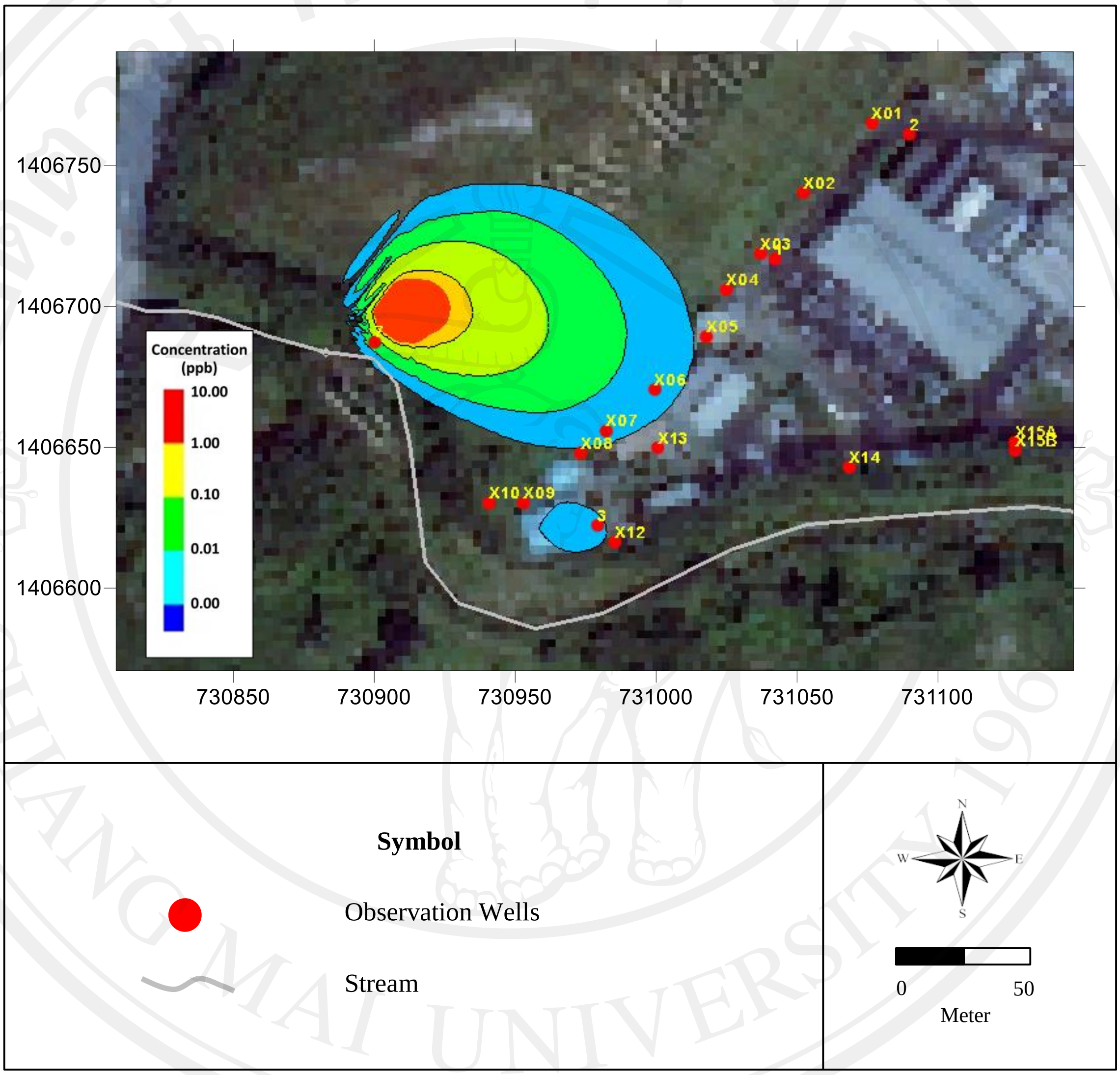


Figure 4.11 Plumes of PCE at the simulated time 27/12/2010 in layer no.3.

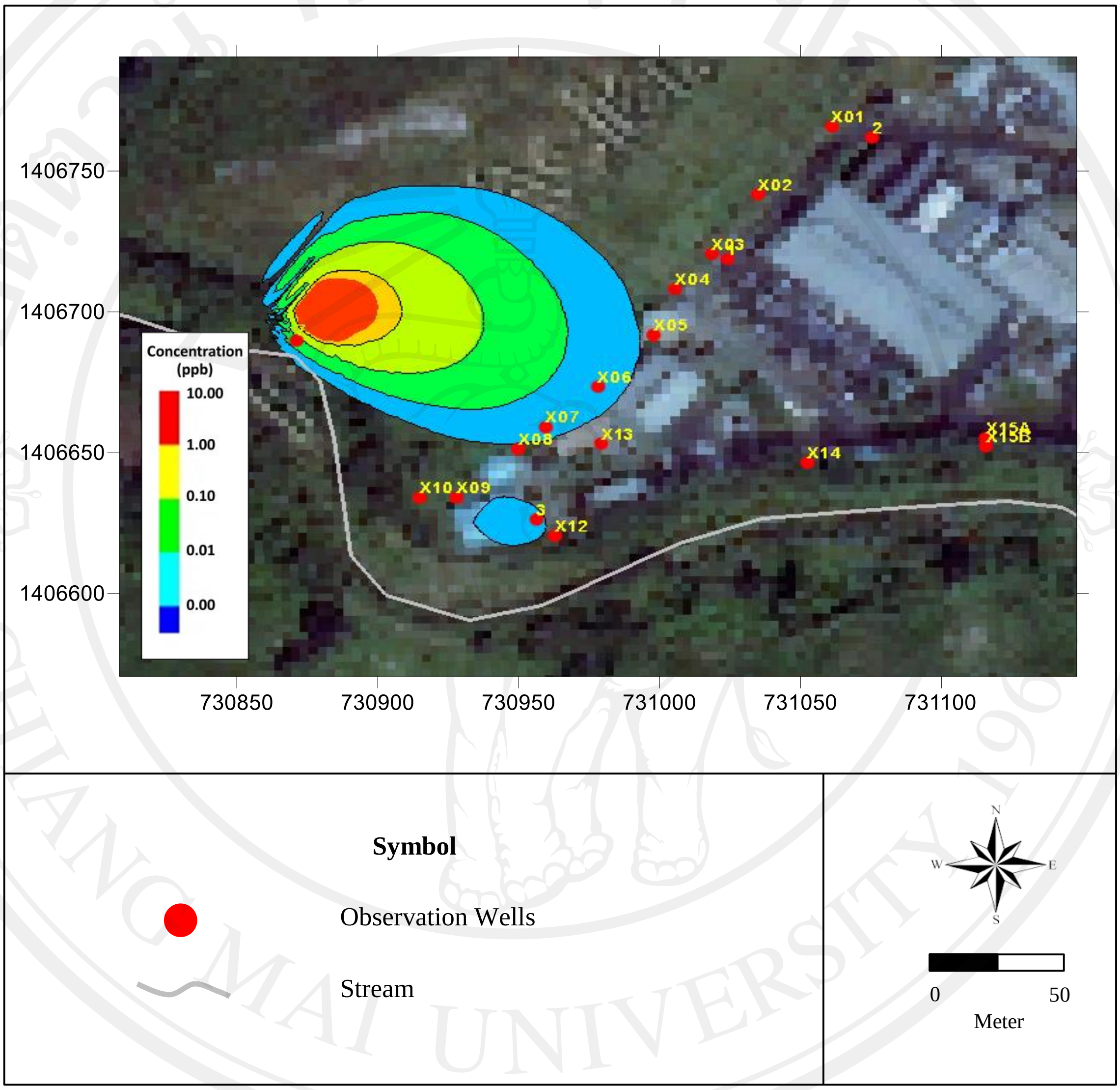


Figure 4.12 Plumes of TCE at the simulated time 27/12/2008 in layer no.3.

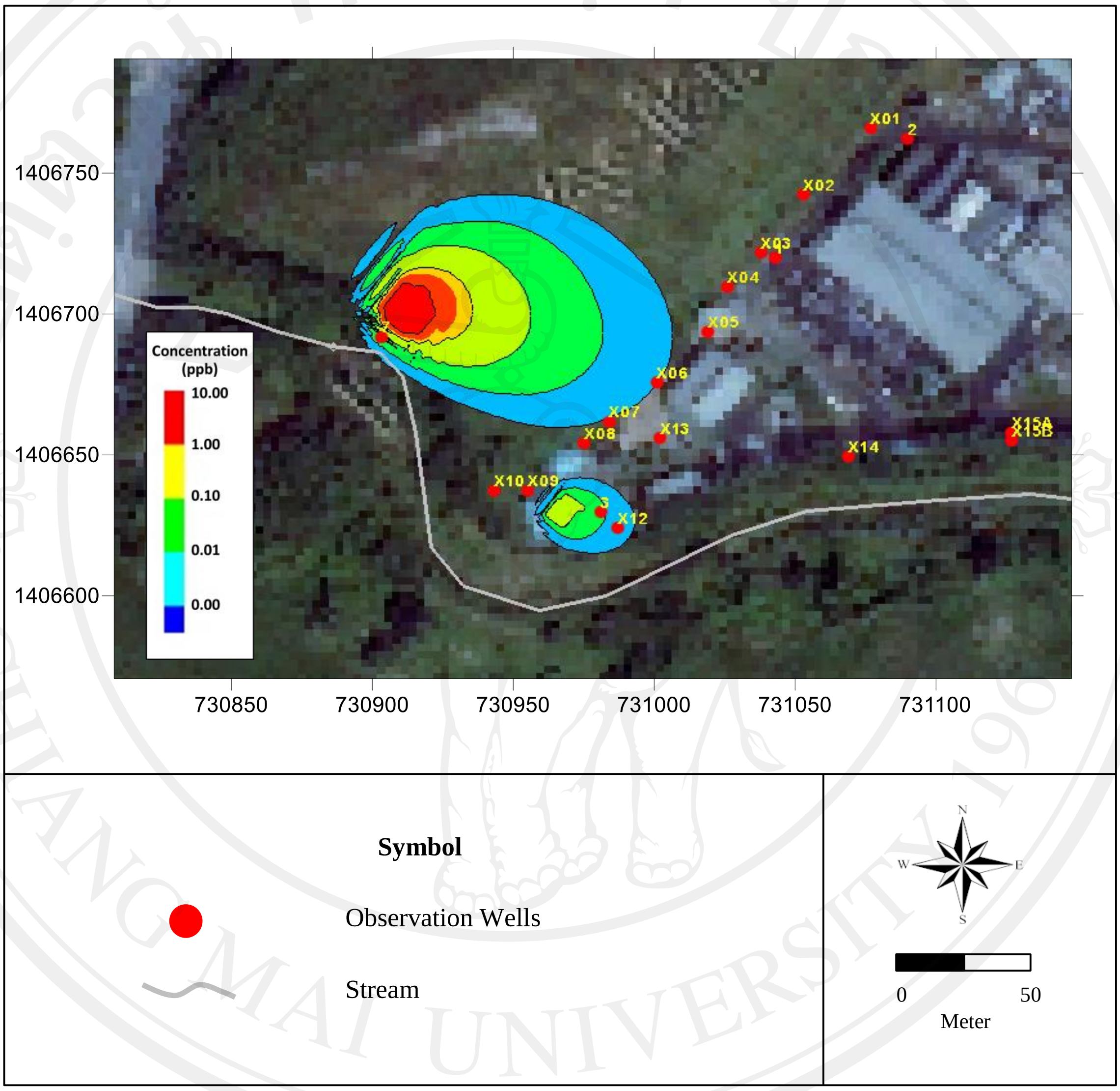


Figure 4.13 Plumes of TCE at the simulated time 27/12/2010 in layer no.3.

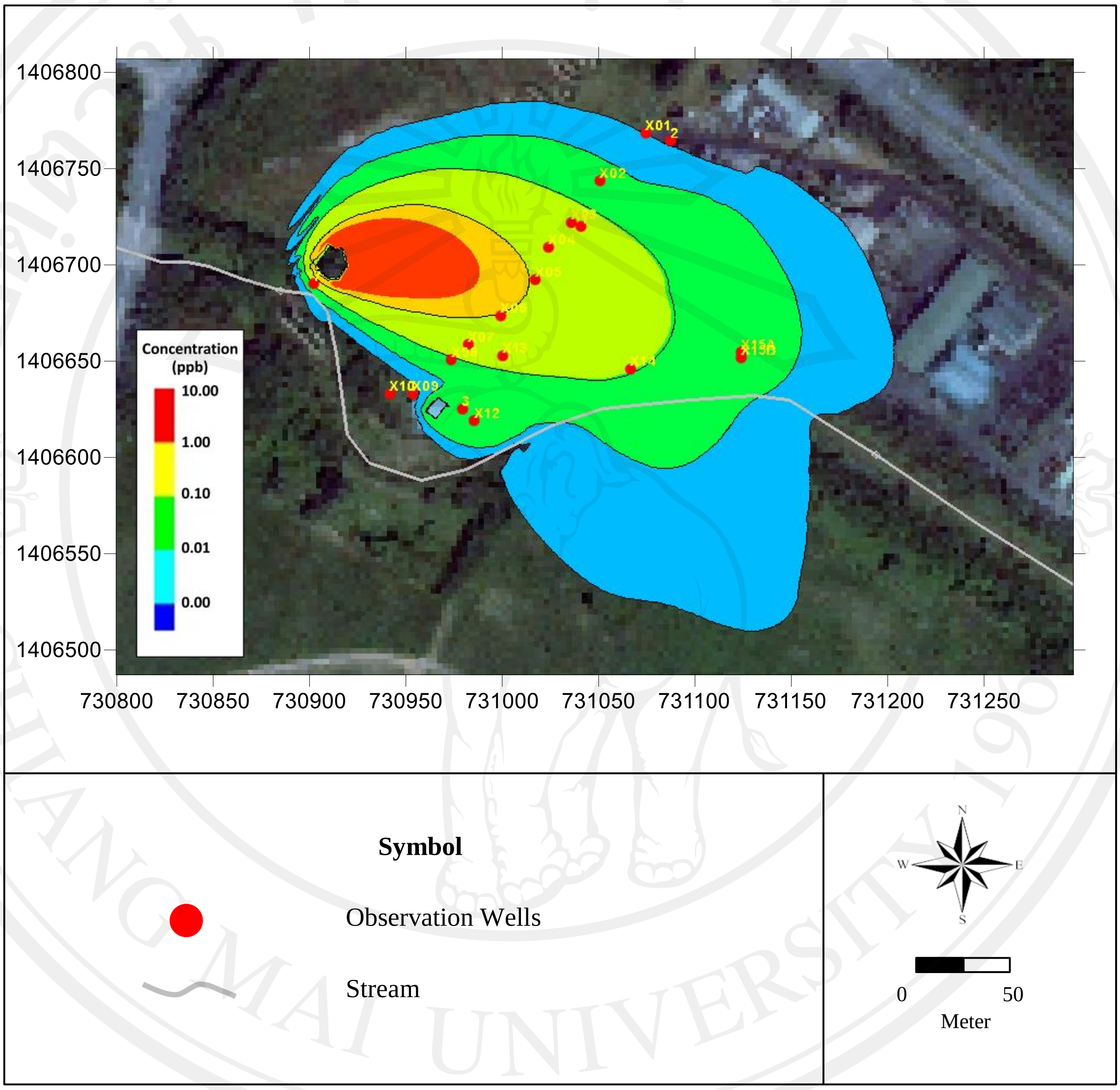


Figure 4.14  Plumes of DCE at the simulated time 27/12/2008 in layer no.3.

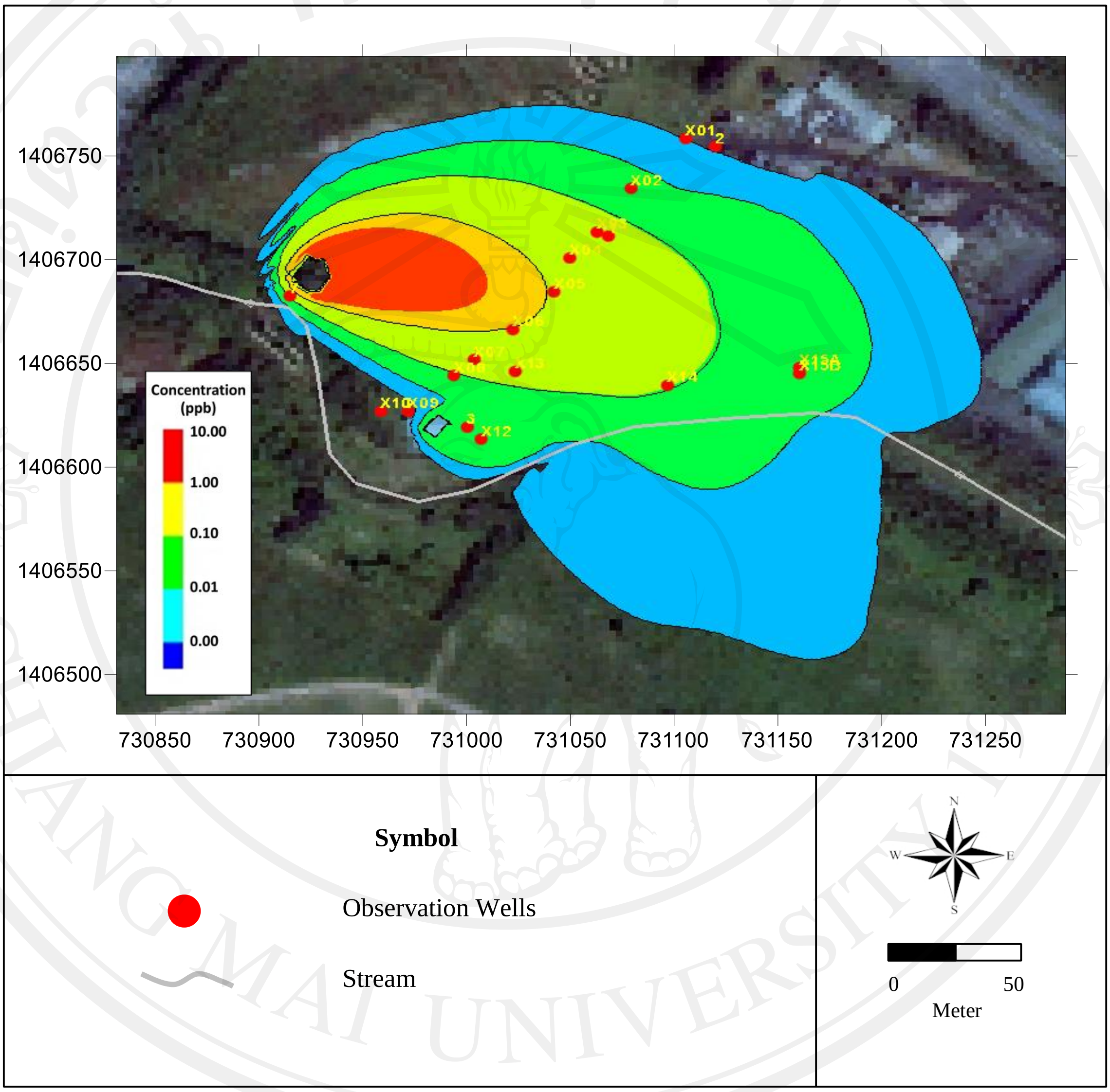


Figure 4.15 Plumes of DCE at the simulated time 27/12/2010 in layer no.3.